Conserved GYXLI motif of FlhA is involved in dynamic domain motions of FlhA required for flagellar protein export

Tohru Minamino[a], Miki Kinoshita[a], Yumi Inoue[a,*], Akio Kitao[b] and Keiichi Namba[a,c,d]

[a]Graduate School of Frontier Biosciences, Osaka University, 1-3 Yamadaoka, Suita, Osaka 565-0871, Japan

[b]School of Life Science and Technology, Tokyo Institute of Technology, 2-12-1 Ookayama, Meguro, Tokyo 152-8550, Japan

[c]RIKEN Center for Biosystems Dynamics Research and SPring-8 Center, 1-3 Yamadaoka, Suita, Osaka 565-0871, Japan

[d]JEOL YOKOGUSHI Research Alliance Laboratories, Osaka University, 1-3 Yamadaoka, Suita, Osaka 565-0871, Japan

Running title: Role of Gly-368 of FlhA in flagellar assembly

[†]Present address: Department of Ophthalmology and Visual Sciences, Kyoto University Graduate School of Medicine, Kyoto, 606-8507 Japan

Address correspondence to Tohru Minamino, tohru@fbs.osaka-u.ac.jp

ABSTRACT

Flagellar structural subunits are transported via the flagellar type III secretion system (fT3SS) and assemble at the distal end of the growing flagellar structure. The C-terminal cytoplasmic domain of FlhA ($FlhA_C$) serves as a docking platform for export substrates and flagellar chaperones and plays an important role in hierarchical protein targeting and export. $FlhA_C$ consists of domains D1, D2, D3, and D4 and adopts open and closed conformations. Gly-368 of *Salmonella* FlhA is located within the highly conserved GYXLI motif and is critical for the dynamic domain motions of $FlhA_C$. However, it remains unclear how it works. Here, we report that periodic conformational changes of the GYXLI motif induce a remodeling of hydrophobic side-chain interaction networks in $FlhA_C$ and promotes the cyclic open-close domain motions of $FlhA_C$. The temperature-sensitive *flhA(G368C)* mutation stabilized a completely closed conformation at 42ºC through strong hydrophobic interactions between Gln-498 of domain D1 and Pro-667 of domain D4 and between Phe-459 of domain D2 and Pro-646 of domain D4, thereby inhibiting flagellar protein export by the fT3SS. Its intragenic suppressor mutations reorganized the hydrophobic interaction networks in the closed $FlhA_C$ structure, restoring the protein export activity of the fT3SS to a significant degree. Furthermore, the conformational flexibility of the GYXLI motif was critical for flagellar protein export. We propose that the conserved GYXLI

motif acts as a structural switch to induce the dynamic domain motions of FlhA$_C$ required for efficient and rapid protein export by the fT3SS.

IMPORTANCE

Many motile bacteria employ the flagellar type III secretion system (fT3SS) to construct flagella beyond the cytoplasmic membrane. The C-terminal cytoplasmic domain of FlhA ($FlhA_C$), a transmembrane subunit of the fT3SS, provides binding-sites for export substrates and flagellar export chaperones to coordinate flagellar protein export with assembly. $FlhA_C$ undergoes cyclic open-close domain motions. The highly conserved Gly-368 residue of FlhA is postulated to be critical for dynamic domain motions of $FlhA_C$. However, it remains unknown how it works. Here, we carried out mutational analysis of $FlhA_C$ combined with molecular dynamics simulation and provide evidence that the conformational flexibility of $FlhA_C$ by Gly-368 is important for remodeling hydrophobic side-chain interaction networks in $FlhA_C$ to facilitate its cyclic open-close domain motions, allowing the fT3SS to transport flagellar structural subunits for efficient and rapid flagellar assembly.

KEYWORDS Bacterial flagellum, flagellar assembly, FlhA, molecular dynamics simulation, type III secretion system, *Salmonella*

INTRODUCTION

Many motile bacteria utilize flagella to swim in viscous liquids and move around on solid surfaces to migrate towards more favorable environments for their survival. The flagellum of *Salmonella enterica* serovar Typhimurium (hereafter referred to as *Salmonella*) is divided into three structural parts: the basal body, which acts as a bi-directional rotary motor; the filament, which functions as a helical propeller to produce thrust; and the hook, which is a universal joint connecting the basal body and filament and transmits torque produced by the motor to the filament. Flagellar assembly begins with the basal body, followed by the hook and finally the filament. To construct the flagellum on the cell surface, the flagellar type III secretion system (fT3SS) transports flagellar structural subunits from the cytoplasm to the distal end of the growing flagellar structure (1).

The fT3SS is located at the base of the flagellum and is composed of a transmembrane export gate complex with a stoichiometry of 9 FlhA, 1 FlhB, 5 FliP, 4 FliQ, and 1 FliR, and a cytoplasmic ATPase ring complex with a stoichiometry of 12 FliH, 6 FliI, and 1 FliJ (Fig. S1A in the Supplemental material). In addition, FlgN, FliS, and FliT act as export chaperones that escort their cognate substrates from the cytoplasm to the fT3SS (2,3). The export gate complex utilizes the transmembrane electrochemical gradient of protons (H^+) as the energy source to unfold and translocate export substrates across the cytoplasmic membrane (4,5). The export gate complex requires ATP hydrolysis by the cytoplasmic ATPase ring complex to become an active

1 H^+/protein antiporter that couples H^+ flow with protein translocation (6–8). The fT3SS
2 also has a Na^+-powered backup engine to maintain the flagellar assembly process
3 when the cytoplasmic ATPase ring complex does not function properly (9,10).

4 *Salmonella* FlhA is composed of an N-terminal transmembrane domain with eight
5 transmembrane helices ($FlhA_{TM}$, residues 1–327), a compactly folded cytoplasmic
6 domain ($FlhA_C$, residues 362–692) and a flexible linker ($FlhA_L$, residues 328–361)
7 connecting these two domains (11,12) (Fig. S1B). $FlhA_{TM}$ acts as a dual-ion channel
8 that conducts both H^+ and Na^+. An interaction between $FlhA_L$ and FliJ activates the ion
9 channel of $FlhA_{TM}$, allowing the export gate complex to couple either H^+ or Na^+ flow
10 with the translocation of export substrate across the cytoplasmic membrane (13).
11 $FlhA_C$ forms a homo-nonamer in the fT3SS (14). The $FlhA_C$ ring serves as a docking
12 platform for export substrates and flagellar chaperones along with the C-terminal
13 cytoplasmic domain of FlhB and plays an important role in hierarchical protein targeting
14 and export for efficient flagellar assembly (15–21).

15 $FlhA_C$ consists of domains D1, D2, D3, and D4 (Fig. S1B) and adopts open and
16 closed conformations (12,22). A highly conserved hydrophobic dimple is located at the
17 interface between domains D1 and D2 and is directly involved in substrate recognition
18 (16,17). Because a large cleft exits in the interface between domains D2 and D4 in the
19 open form of $FlhA_C$, but not in the closed form, the chaperone-substrate complexes
20 can bind to the conserved hydrophobic dimple in the open form but not in the closed
21 form (23,24). For filament assembly, the C-terminal region of $FlhA_L$ binds to domains

1 D1 and D2 of its neighboring $FlhA_C$ subunit in the $FlhA_C$ ring structure to stabilize the
2 open conformation, allowing the chaperones-substrate complexes to efficiently bind to
3 the $FlhA_C$ ring (25). During hook assembly, however, $FlhA_L$ binds to the conserved
4 hydrophobic dimple of the open form not only to suppress premature docking of the
5 chaperone-substrate complexes to $FlhA_C$ but also to facilitate the export of the hook
6 protein FlgE (26). These observations suggest that the open form of $FlhA_C$ reflects an
7 active state of the fT3SS. However, little is known about the role of the closed form of
8 $FlhA_C$ in flagellar protein export.

9 The *flhA(G368C)* mutation inhibits the protein transport activity of the fT3SS at a
10 restrictive temperature of 42ºC but not at a permissive temperature of 30ºC (27–29).
11 The temperature shift-up from 30ºC to 42ºC arrests the export of flagellar proteins by
12 the fT3SS with the *flhA(G368C)* mutation. Molecular dynamics (MD) simulation has
13 shown that the *flhA(G368C)* mutation restricts cyclic open-close domain motions of
14 $FlhA_C$ at 42ºC and stabilizes a completely closed conformation of $FlhA_C$ (24). Gly-368
15 is located within the highly conserved GYXLI motif (Fig. 1A). This leads to a plausible
16 hypothesis that the conserved GYXLI motif may be critical for such domain motions of
17 $FlhA_C$ coupled with flagellar protein export.

18 To clarify this hypothesis, we carried out mutational analysis of $FlhA_C$ combined
19 with MD simulation. We provide evidence that the *flhA(G368C)* mutation stabilizes
20 hydrophobic side-chain interactions between domains D1 and D3 and those between
21 domains D2 and D4, thereby suppressing dynamic open-close domain motions of

1 $FlhA_C$, and that its intragenic suppressor mutations induce the remodeling of the
2 hydrophobic interaction networks in $FlhA_C$, allowing $FlhA_C$ with the G368C mutation
3 ($FlhA_{C\text{-}G368C}$) to restore the dynamic open-close domain motions.
4
5 ## RESULTS
6 **Effect of *flhA(G368C)* mutation on hydrophobic side-chain interaction networks**
7 **in $FlhA_C$.** To address why the *flhA(G368C)* mutation stabilizes a completely closed
8 form of $FlhA_C$ at 42ºC, we first compared the interfaces between domains D1 and D3
9 and those between domains D2 and D4 in the open and closed forms of $FlhA_{C\text{-}G368C}$
10 obtained by MD simulation (Fig. 1B). Met-398 and Gln-498 of domain D1 make
11 hydrophobic contacts with Pro-550 of domain D3 and Pro-667 of domain D4,
12 respectively (left panel). Phe-459 of domain D2 makes a hydrophobic contact with Pro-
13 646 of domain D4 (left panel). Because the hydrophobic interactions between Phe-459
14 and Pro-646 and those between Gln-498 and Pro-667 are not seen in the open form
15 of $FlhA_{C\text{-}G368C}$ (right panel), we suggest that the *flhA(G368C)* mutation stabilizes these
16 two hydrophobic interactions at 42ºC, thereby suppressing cyclic open-close motions
17 of $FlhA_C$.
18
19 **MD simulation of $FlhA_C$ with either G368C/K548C or G368C/F459C/K548C**
20 **mutation.** The highly conserved Lys-548 residue of FlhA is located at the interface
21 between domains D1 and D3 and contributes to D1-D3 interactions (12) (Fig. 1B). The

1 *flhA(K548C)* mutation in domain D3 does not affect FlhA function at all. However, the
2 combination of *flhA(G368C)* and *flhA(K548C)* mutations results in a loss-of-function
3 phenotype even at 30ºC (Fig. 2A) (24). To clarify why the *flhA(G368C/K548C)* mutation
4 inhibits flagellar protein export at 30ºC, we analyzed the structure and dynamics of
5 $FlhA_{C\text{-}G368C/K548C}$ by MD simulation at 30ºC for 1.5 μs. Domains D1 and D2 behaved as
6 a rigid body in all cases. In contrast, domain D4 became closer to domain D2 through
7 conformational changes of two hinges, one between domains D1 and D3 and the other
8 between domains D3 and D4, when $FlhA_C$ switched from an open conformation to a
9 closed conformation. Therefore, we calculated the center-of-mass distance (d_{24})
10 between domains D2 and D4 during MD simulation (Fig. 2B).
11 Unlike $FlhA_{C\text{-}G368C}$, which changes its conformation back and forth between the
12 closed and open forms at 30ºC (24), $FlhA_{C\text{-}G368C/K548C}$ stopped the dynamic domain
13 motions at 30ºC after 0.3 μs and switched its conformation to a completely closed form
14 (Fig. 2B). When we compared the fully closed form of $FlhA_{C\text{-}G368C/K548C}$ with that of
15 $FlhA_{C\text{-}G368C}$, there was a significant difference in the orientation of domain D4 relative
16 to domain D3 (Fig. 2C, left panel). Unlike $FlhA_{C\text{-}G368C}$, in which hydrophobic interactions
17 between Gln-498 and Pro-667 and those between Phe-459 and Pro-646 stabilize the
18 closed conformation of $FlhA_{C\text{-}G368C}$ (Fig. 1B, left panel), the hydrophobic interactions of
19 Pro-667 with Phe-459 and Leu-461 locked the $FlhA_{C\text{-}G368C/K548C}$ structure into the fully
20 closed conformation at 30ºC (Fig. 2D).

1 It has been reported that the *flhA(F459C)* mutation restores motility of the
2 *flhA(G368C/K548C)* mutant to a considerable degree (Fig. 2A) (24), we analyzed the
3 effect of this mutation on the structure and dynamics of $FlhA_{C\text{-}G368C/K548C}$ by MD
4 simulation. The F459C substitution restored the dynamic open-close domain motions
5 of $FlhA_{C\text{-}G368C/K548C}$ at 30ºC (Fig. 2B). $FlhA_{C\text{-}G368C/F459C/K548C}$ also adopted a super-open
6 conformation (Fig. 2C, right panel) as seen in the wild-type structure at 42ºC (24).
7 Therefore, we conclude that the cyclic open-close domain motion of $FlhA_C$ is required
8 for efficient export of flagellar structural subunits by the fT3SS and that the completely
9 closed form of $FlhA_C$ reflects an inactive state of the fT3SS.
10
11 **Isolation of pseudorevertants from the *flhA(G368C/K548C)* mutant.** To clarify how
12 the *flhA(G368C/K548C)* double mutation locks $FlhA_C$ into the fully closed conformation
13 at 30ºC, pseudorevertants were isolated from the *flhA(G368C/K548C)* mutant by
14 streaking an overnight culture out on 0.35% soft agar plates, incubating them at 30ºC
15 for a few days and looking for motility halos emerging from the streak. In total five
16 motile colonies were purified from such halos. The motility of these pseudorevertants,
17 as illustrated with MMA2228KC-01 [*flhA(M365I/G368C/K548C)*] and MMA2228KC-03
18 [*flhA(G368C/A446E/K548C)*], was better than that of the *flhA(G368C/K548C)* strain at
19 30ºC (Fig. S2A in the Supplemental material). Consistently, the secretion levels of FlgD
20 (hook capping protein), FlgK (hook-filament junction protein), and FliC (filament protein,
21 flagellin) by these pseudorevertants were higher than those by the *flhA(G368C/K548C)*

mutant (Fig. S2B). All suppressor mutations were identified in $FlhA_C$: M365I and R370S (isolated twice) in domain D1; A446E in domain D2; and P550S in domain D3 (Fig. 1B). These four mutations have also been isolated as gain-of-function mutations that restore the motility defect of the *flhA(G368C)* mutant at 42ºC (28,29). Because Gly-368 is located structurally far from Lys-548 (Fig. 1B), we hypothesize that the *flhA(G368C)* mutation may induce remodeling of the hydrophobic side-chain interaction networks in $FlhA_C$, thereby inhibiting the dynamic open-close domain motions in $FlhA_{C\text{-}G368C/K548C}$.

Effect of *flhA(G368C)* and its intragenic suppressor mutations on the hydrophobic side-chain interaction networks. There were structural differences in domains D1 and D2 when the open and closed forms of $FlhA_{C\text{-}G368C}$ were compared (Fig. S3 in the Supplemental material). Gly-368 forms the highly conserved GYXLI motif along with Tyr-369, Arg-370, Leu-371, and Ile-372 (Fig. 1A), which forms a short α-helix (Fig. S3). Cys-368 of $FlhA_{C\text{-}G368C}$ made much stronger hydrophobic contacts with Arg-370, Leu-413 and Pro-415 of domain D1 in the completely closed form than in its open form (Fig. 3A). As a result, the G368C mutation induced a significant conformational change of this α-helix (Fig. S3). The R370S suppressor mutation is located within the conserved GYXLI motif (Fig. 1A) and presumably weakened the strong hydrophobic interactions among Cys-368, Leu-413 and Pro-415 (Fig. 3A), thereby partially restoring the protein export activity of the fT3SS with the G368C

1 substitution. Therefore, we propose that the conserved GYXLI motif may act as a
2 structural switch to induce the cyclic open-close domain motion of $FlhA_C$.
3 To clarify how the *flhA(G368C)* mutation stabilizes the completely closed form of
4 $FlhA_C$ at 42ºC through the strong hydrophobic interactions between Gln-498 and Pro-
5 667 and those between Phe-459 and Pro-646, we next analyzed the effect of the
6 M365I, A446E, and P550S suppressor mutations on the conformational changes of
7 $FlhA_{C\text{-}G368C}$. Met-365 of domain D1 made a strong hydrophobic contact with Leu-492
8 of domain D1 in the closed form of $FlhA_{C\text{-}G368C}$ but not in its open form (Fig. 3B).
9 Therefore, the M365I substitution must have affected this hydrophobic interaction to
10 induce the conformational change of domain D1, thereby weakening the hydrophobic
11 interaction between Gln-498 and Pro-667 in $FlhA_{C\text{-}G368C}$. Ala-446 of domain D2
12 hydrophobically interacted with Gln-477 of domain D2 in both open and closed forms
13 of $FlhA_{C\text{-}G368C}$ (Fig. 3C), and so the A446E mutation would induce the formation of a
14 hydrogen bond between Glu-446 and Gln-447 as well as a hydrophobic contact. As a
15 result, this mutation may induce a conformational change of domain D2, affecting the
16 hydrophobic contact between Phe-459 and Pro-646. Pro-550 of domain D3 makes a
17 hydrophobic contact with Met-398 of domain D1 (Fig. 1B), and therefore the P550S
18 substitution should weaken the hydrophobic interactions between domains D1 and D3.
19 Taken all together, we hypothesize that a conformational change of the conserved
20 GYXLI motif may induce a remodeling of hydrophobic side-chain interaction networks
21 in $FlhA_C$ required for its dynamic open-close domain motion.

1

2 **Mutational analysis of residues forming hydrophobic side-chain interaction**

3 **networks in FlhA$_{C\text{-}G368C}$.** To test whether the *flhA(G368C)* mutation affects the

4 hydrophobic side-chain interaction networks in FlhA$_C$, we constructed *flhA(G368C)*

5 mutants with either L413A, P415A, P434A, F459A, Q477A, L492A, Q498A, K548A,

6 P646A or P667A substitution and analyzed the motility of these double mutants at both

7 30ºC and 42ºC (Fig. 4A). These double mutations did not affect the steady expression

8 level of FlhA as judged by immunoblotting with polyclonal anti-FlhA$_C$ antibody (Fig. 4B),

9 The P415A, P434A, Q477A, Q498A, and K548A substitutions reduced the

10 motility of the *flhA(G368C)* mutant even at 30ºC (Fig. 4A). Consistently, these five

11 substitutions reduced the secretion levels of FlgD and FlgK by the fT3SS (Fig. 4B).

12 Furthermore, they considerably reduced the motility of the *flhA(G368C)* mutant at 42ºC

13 (Fig. 4A). The P415A, P434A, Q477A, Q498A and K548A substitutions themselves

14 displayed no phenotype at both 30ºC and 42ºC (Fig. 5A). Therefore, we conclude that

15 the *flhA(G368C)* mutation affects the hydrophobic side-chain interaction networks in

16 FlhA$_C$, thereby inducing conformational changes of domains D1 and D2.

17 The L413A and L492A substitutions interfered with the motility of the *flhA(G368C)*

18 mutant at both 30ºC and 42ºC (Fig. 4A). Consistently, these two substitutions inhibited

19 the secretion of both FlgD and FlgK by the *flhA(G368C)* mutant grown at 30ºC (Fig.

20 4B). The L413A mutation itself did not inhibit motility at either 30ºC or 42ºC (Fig. 5A,

21 upper panels). Because Cys-368 makes strong hydrophobic contacts with Arg-370,

1 Leu-413 and Pro-415 of domain D1 in the completely closed form of $FlhA_{C\text{-}G368C}$ (Fig.
2 3A), we suggest that the L413A mutation stabilizes these hydrophobic contacts even
3 at 30ºC, thereby inhibiting the protein transport activity of the fT3SS. In contrast to the
4 L413A mutation, the L492A substitution itself significantly reduced motility at 42ºC but
5 not at 30ºC (Fig. 5A, lower panels). Consistently, this substitution inhibited the
6 secretion of FlgD and FlgK by the fT3SS at 42ºC but not at 30ºC (Fig. 5B). These
7 results indicate that the temperature shift-up from 30ºC to 42ºC induces a
8 conformational change of domain D1 of $FlhA_C$ by the L492A substitution, thereby
9 reducing the protein export activity of the fT3SS. Because Leu-492 makes a
10 hydrophobic contact with Met-365 in the closed form of $FlhA_{C\text{-}G368C}$ but not in its open
11 form (Fig. 3B), we suggest that a proper switching of the hydrophobic side-chain
12 interaction between Met-365 and Leu-492 is critical for flagellar protein export by the
13 fT3SS.

14 Phe-459 of FlhA is located within a highly conserved hydrophobic dimple at the
15 interface between domains D1 and D2 (Fig. 1B) and is directly involved in substrate
16 recognition (16,17,23,24). The F459A mutation reduced the motility of the *flhA(G368C)*
17 mutant at both 30ºC and 42ºC (Fig. 4A, upper panels). This mutation reduced the level
18 of FlgK secretion by the *flhA(G368C)* mutant grown at 30ºC but not the level of FlgD
19 secretion (Fig. 4B), indicating that the F459A substitution affects the docking of the
20 FlgN-FlgK chaperone-export substrate complex to $FlhA_{C\text{-}G368C}$ but not that of FlgD, in
21 agreement with previous reports (17,21). Because the motility of the

1 *flhA(G368C/F459A)* was much worse than that of the *flhA(F459A)* mutant (Figs. 4 and
2 5), we suggest that the G368C mutation induces a conformational change of the
3 conserved hydrophobic dimple involved in the interaction with flagellar chaperones.
4 Furthermore, the temperature shift-up from 30ºC to 42ºC reduced the levels of both
5 FlgD and FlgK secretion by the *flhA(F459A)* mutant (Fig. 5B), thereby reducing motility
6 at 42ºC (Fig. 5A). Therefore, we propose that a remodeling of hydrophobic side-chain
7 interaction networks in the conserved hydrophobic dimple may be required for efficient
8 and stable binding of export substrates and chaperone-substrate complexes to $FlhA_C$.
9 The P646A and P667A mutations, which are located within domain D4, did not
10 affect the motility of the *flhA(G368C)* mutant at both 30ºC and 42ºC (Fig 3A, lower
11 panels). These two mutations themselves showed no phenotype (Fig4A, lower panels),
12 indicating that these two proline residues are not critical for the FlhA function. The
13 structural transition from the open conformation to the closed conformation occurs in
14 at least two steps (24). The first conformational change occurs at the interface between
15 domains D3 and D4, resulting in a 13° rotation of domain D4 in the direction towards
16 domain D2, and the second conformational change occurs at a flexible hinge between
17 domains D1 and D3, allowing $FlhA_C$ to adopt the closed form. Therefore, we suggest
18 that the *flhA(G368C)* mutation limits the hinge movement between domains D1 and
19 D3 through a remodeling of the hydrophobic side-chain interaction networks of domain
20 D1, thereby allowing Pro-646 and Pro-667 to make the strong hydrophobic contacts
21 with Phe-459 and Gln-498, respectively (Fig. 1B).

1

2 ## Discussion

3 The temperature-sensitive *flhA(G368C)* mutation limits the cyclic open-close domain
4 motions of $FlhA_C$ at 42ºC, thereby reducing the flagellar protein export by the fT3SS
5 and therefore the cell motility (24). Gly-368 is located within the highly conserved
6 GYXLI motif of $FlhA_C$ (Fig. 1A). This suggests that the GYXLI motif is involved in such
7 domain motions of $FlhA_C$. To clarify the role of Gly-368 in flagellar protein export, we
8 performed mutational analysis of $FlhA_{C\text{-}G368C}$ combined with MD simulation and
9 showed that the *flhA(G368C)* mutation induced a remodeling of hydrophobic side-
10 chain interaction networks in $FlhA_C$ at 42ºC, allowing Gln-498 of domain D1 and Phe-
11 459 of domain D2 to hydrophobically interact with Pro-667 and Pro-646 of domain D4,
12 respectively (Fig. 1B). As a result, the *flhA(G368C)* mutation not only suppresses the
13 dynamic open-close domain motions of $FlhA_C$ but also stabilizes the completely closed
14 conformation at 42ºC. Its suppressor mutations affected the hydrophobic side-chain
15 interaction networks in the closed $FlhA_C$ structure, thereby restoring the protein export
16 activity of the fT3SS containing the *flhA(G368C)* mutation to a significant degree (Fig.
17 3). Cys-368 hydrophobically interacts with Arg-370, Leu-413 and Pro-415 of domain
18 D1 in the closed form of $FlhA_{C\text{-}G368C}$ but not in its open form (Fig. 3A). Therefore, we
19 conclude that the conformational flexibility of $FlhA_C$ by Gly-368 is required for cyclic
20 conformational changes of the conserved GYXLI motif, allowing $FlhA_C$ to undergo the

1 cyclic open-close domain motions through the remodeling of the hydrophobic side-
2 chain interaction networks in $FlhA_C$.

3 We showed that the completely closed form of $FlhA_C$ reflected an inactive state
4 of the fT3SS and that the cyclic open-close domain motions of $FlhA_C$ was critical for
5 efficient and rapid flagellar protein transport by the fT3SS (Fig. 2). The FlgN, FliS, and
6 FliT chaperones in complex with their cognate substrates bind to $FlhA_C$ at a nanomolar
7 affinity (17,30), and such strong interactions between the chaperones and $FlhA_C$ assist
8 protein unfolding and export by the fT3SS (31,32). The flagellar chaperones bind to
9 the open form of $FlhA_C$ but not to the closed form (23,24). Purified $FlhA_{C\text{-}G368C}$ prefers
10 to adopt a closed conformation even at room temperature (24). Because pull-down
11 assays by GST affinity chromatography have revealed that the *flhA(G368C)* mutation
12 reduces the binding affinity of $FlhA_C$ for the chaperone-substrate complex (24), we
13 propose that the structural transition of $FlhA_C$ from the open to the closed form may
14 induce the dissociation of empty chaperone from $FlhA_C$ for the binding of a newly
15 delivered chaperone-substrate complex for the export of next substrate.

16 FliJ binds to $FlhA_L$ with high affinity and opens both the H^+ and polypeptide
17 channels of the transmembrane export gate complex, allowing the fT3SS to couple H^+
18 flow through the H^+ channel with the translocation of export substrate through the
19 polypeptide channel (Fig. S1B in the Supplemental material) (6,15,26). FliJ also binds
20 to $FlhA_C$ with low affinity (26). It has been shown that CdsO, a FliJ homolog, binds to
21 $CdsV_C$, a $FlhA_C$ homolog, at a large cleft between the D4 domains of neighboring

1 $CdsV_C$ subunits in the $CdsV_C$ ring structure (33). This suggests that FliJ also binds to
2 the cleft between the D4 domains of neighboring $FlhA_C$ subunits in the $FlhA_C$ ring. It
3 has been reported that FliJ stabilizes the interaction between $FlhA_C$ and FliT in complex
4 with FliD (15). This raises the possibility that the interaction of FliJ with the cleft
5 between the D4 domains in the $FlhA_C$ ring may stabilize the open conformation of
6 $FlhA_C$ subunits in the ring. To clarify this possibility, we built the models of the $FlhA_C$
7 ring in complex with FliJ in the open and closed forms of $FlhA_C$ based on the crystal
8 structure of the $CdsV_C$ ring in complex with CdsO (PDB ID: 6WA9) (Fig. 6). FliJ can
9 bind to the cleft between the D4 domains of neighboring $FlhA_C$ subunits stably when
10 $FlhA_C$ adopts the open form in the ring structure (right panel) because FliJ can contact
11 both $FlhA_C$ subunits. However, the FliJ binding to of $FlhA_C$ in the closed form appears
12 to be unstable (left panel) because the distance between the neighboring D4 domains
13 is longer in the closed form than that in the open form, restraining the proper contacts
14 of FliJ with two $FlhA_C$ subunits (middle panel). Because the open and closed forms of
15 $FlhA_C$ represent the active and inactive states of the fT3SS, respectively (Fig. 2), we
16 propose that the cyclic open-close domain motion of $FlhA_C$ is important for efficient and
17 robust energy coupling mechanism of the fT3SS.
18

19 ## MATERIALS AND METHODS

20 **Bacterial strains, P22-mediated transduction and DNA manipulations.** *Salmonella*
21 strains used in this study are listed in Table 1. P22-mediated transductional crosses

1 were performed with P22HT*int* (34). DNA manipulations were performed using
2 standard protocols. Site-directed mutagenesis was carried out using Prime STAR Max
3 Premix as described in the manufacturer's instructions (Takara Bio). All of the *flhA*
4 mutations were confirmed by DNA sequencing (Eurofins Genomics).
5
6 **Motility assay.** Fresh colonies were inoculated onto soft agar plates [1% (w/v) triptone,
7 0.5% (w/v) NaCl, 0.35% (w/v) Bacto agar], and then the plates were incubated at 30°C.
8
9 **Secretion assay.** *Salmonella* cells were grown in 5 ml of L-broth [1% (w/v) Bacto-
10 tryptone, 0.5% (w/v) Bacto-yeast extract, 0.5% (w/v) NaCl] at either 30ºC or 42ºC with
11 shaking until the cell density reached an OD_{600} of ca. 1.2–1.4. Cultures were
12 centrifuged to obtain cell pellets and culture supernatants. The cell pellets were
13 resuspended in sodium dodecyl sulfate (SDS)-loading buffer solution [62.5 mM Tris-
14 HCl, pH 6.8, 2% (w/v) SDS, 10% (w/v) glycerol, 0.001% (w/v) bromophenol blue]
15 containing 1 µl of 2-mercaptoethanol. Proteins in the culture supernatants were
16 precipitated by 10% trichloroacetic acid and suspended in a Tris/SDS loading buffer
17 (one volume of 1 M Tris, nine volumes of 1 X SDS-loading buffer solution) containing
18 1 µl of 2-mercaptoethanol (35). Both whole cellular proteins and culture supernatants
19 were normalized to a cell density of each culture to give a constant number of
20 *Salmonella* cells. After boiling proteins in both whole cellular and culture supernatant
21 fractions at 95ºC for 3 min, these protein samples were separated by SDS–

polyacrylamide gel electrophoresis and transferred to nitrocellulose membranes (Cytiva) using a transblotting apparatus (Hoefer). Then, immunoblotting with polyclonal anti-FlgD, anti-FlgK, anti-FliC or anti-$FlhA_C$ antibody was carried using iBind Flex Western Device (Thermo Fisher Scientific) as described in the manufacturer's instructions. Detection was performed with Amersham ECL Prime western blotting detection reagent (Cytiva). Chemiluminescence signals were captured by a Luminoimage analyzer LAS-3000 (GE Healthcare). At least three measurements were performed.

Multiple sequence alignment. Multiple sequence alignment was carried out using CLUSTAL-Ω (http://www.ebi.ac.uk/Tools/msa/clustalo/).

MD simulation. MD simulations of $FlhA_C$ with either G368C/K548C or G368C/F459C/K548C substitution were conducted as described previously (24). The mutant structures were constructed based on the 3A5I structure of $FlhA_C$ (12). AMBER ff14SB force field (36) was used for the proteins. Each mutant was initially solvated in a cubic box of SPC/E_b water molecules (37) and 0.17 M KCl (38) with a margin of at least 12 Å from the proteins to the periodic box boundaries. The simulation was conducted with the *pmemd.cuda* module (39) of AMBER20/21 (40). MD simulations of the G368C/K548C and G368C/F459C/K548C mutants were independently conducted at 300 K. After energy minimization and equilibration MD for 1 ns with positional

restraints for the protein main chain atoms at 300 K and 1 atm, MD simulation without restraints were conducted for 1.5 μs.

ACKNOWLEDGEMENTS

This work was supported in part by JSPS KAKENHI Grant Numbers JP20K15749 (to M.K.), JP19H03191, JP20H05439, and JP21H05510 (to A.K.), and JP19H03182 (to T.M.). This work has also been supported by Platform Project for Supporting Drug Discovery and Life Science Research (BINDS) from AMED under Grant Number JP19am0101117 to K.N., by the Cyclic Innovation for Clinical Empowerment (CiCLE) from AMED under Grant Number JP17pc0101020 to K.N. and by JEOL YOKOGUSHI Research Alliance Laboratories of Osaka University to K.N.

REFERENCES

1. Nakamura S, Minamino T. 2019. Flagella-driven motility of bacteria. Biomolecules 9:279.
2. Minamino T. 2014. Protein export through the bacterial flagellar type III export pathway. Biochim Biophys Acta 1843:1642–1648.
3. Minamino T, Kawamoto A, Kinoshita M, Namba K. 2020. Molecular organization and assembly of the export apparatus of flagellar type III secretion systems. Curr Top Microbiol Immunol 427:91–107.

4. Minamino T, Namba K. 2008. Distinct roles of the FliI ATPase and proton motive force in bacterial flagellar protein export. Nature 451:485–488.
5. Paul K, Erhardt M, Hirano T, Blair DF, Hughes KT. 2008. Energy source of flagellar type III secretion. Nature 451:489–492.
6. Minamino T, Morimoto YV, Hara N, Namba K. 2011. An energy transduction mechanism used in bacterial type III protein export. Nat Commun 2:475 (2011).
7. Morimoto YV, Kami-ike N, Miyata T, Kawamoto A, Kato T, Namba K, Minamino T. 2016. High-resolution pH imaging of living bacterial cell to detect local pH differences. mBio 7:01911-16.
8. Minamino T, Morimoto YV, Kinoshita, M., Aldridge PD, Namba K. 2014. The bacterial flagellar protein export apparatus processively transports flagellar proteins even with extremely infrequent ATP hydrolysis. Sci Rep 4:7579.
9. Minamino T, Morimoto YV, Hara N, Aldridge PD, Namba K. 2016. The bacterial flagellar type III export gate complex is a dual fuel engine that can use both H^+ and Na^+ for flagellar protein export. PLOS Pathog 12:e1005495.
10. Minamino T, Kinoshita M, Morimoto YV, Namba K. 2021. The FlgN chaperone activates the Na^+-driven engine of the *Salmonella* flagellar protein export apparatus. Commun Biol 4:335.
11. Minamino T, Iino T, Kutsukake K. 1994. Molecular characterization of the *Salmonella typhimurium flhB* operon and its protein products. J Bacteriol 176:7630–7637.

12. Saijo-Hamano Y, Imada K, Minamino T, Kihara M, Shimada M, Kitao A, Namba K. 2010. Structure of the cytoplasmic domain of FlhA and implication for flagellar type III protein export. Mol Microbiol 76:260–268 (2010).
13. Minamino T, Morimoto YV, Kinoshita M, Namba K. 2021. Membrane voltage-dependent activation mechanism of the bacterial flagellar protein export apparatus. Proc Natl Acad Sci USA 118:e2026587118.
14. Abrusci P, Vergara-Irigaray M, Johnson S, Beeby MD, Hendrixson DR, Roversi P, Friede ME, Deane JE, Jensen GJ, Tang CM, Lea SM. 2013. Architecture of the major component of the type III secretion system export apparatus. Nat Struct Mol Biol 20:99–104.
15. Bange G, Kümmerer N, Engel C, Bozkurt G, Wild K, Sinning I. 2010. FlhA provides the adaptor for coordinated delivery of late flagella building blocks to the type III secretion system. Proc Natl Acad Sci USA 107:11295–11300.
16. Minamino T, Kinoshita M, Hara N, Takeuchi S, Hida A, Koya S, Glenwright H, Imada K, Aldridge PD, Namba K. 2012. Interaction of a bacterial flagellar chaperone FlgN with FlhA is required for efficient export of its cognate substrates. Mol Microbiol 83:775–788.
17. Kinoshita M, Hara N, Imada K, Namba K, Minamino, T. 2013. Interactions of bacterial chaperone-substrate complexes with FlhA contribute to co-ordinating assembly of the flagellar filament. Mol Microbiol 90:1249–1261.

18. Minamino T, Inoue Y, Kinoshita M, Namba K. 2020. FliK-driven conformational rearrangements of FlhA and FlhB are required for export switching of the flagellar protein export apparatus. J Bacteriol 202:e00637-19.

19. Kinoshita M, Namba K, Minamino T. 2021. A positive charge region of *Salmonella* FliI is required for ATPase formation and efficient flagellar protein export. Commun Biol 4:464.

20. Minamino T, Kinoshita M, Inoue Y, Morimoto YV, Ihara K, Koya S, Hara N, Nishioka N, Kojima S, Homma M, Namba K. 2016. FliH and FliI ensure efficient energy coupling of flagellar type III protein export in *Salmonella*. MicrobiologyOpen 5:424–435.

21. Inoue Y, Morimoto YV, Namba K, Minamino T. 2018. Novel insights into the mechanism of well-ordered assembly of bacterial flagellar proteins in *Salmonella*. Sci Rep 8:1787.

22. Moore SA, Jia Y. 2010. Structure of the cytoplasmic domain of the flagellar secretion apparatus component FlhA from *Helicobacter pylori*. J Biol Chem 285:21060–21069.

23. Xing Q, Shi K, Portaliou A, Rossi P, Economou A, Kalodimos CG. 2018. Structure of chaperone-substrate complexes docked onto the export gate in a type III secretion system. Nat Commun 9:1773.

24. Inoue Y, Ogawa Y, Kinoshita M, Terahara N, Shimada M, Kodera N, Ando T, Namba K, Kitao A, Imada K, Minamino T.2019. Structural insight into the substrate

specificity switching mechanism of the type III protein export apparatus. Structure 27:965–976.

25. Terahara N, Inoue Y, Kodera N, Morimoto YV, Uchihashi T, Imada K, Ando T, Namba K, Minamino T. 2018. Insight into structural remodeling of the FlhA ring responsible for bacterial flagellar type III protein export. Sci Adv 4:eaao7054.

26. Inoue Y, Kinoshita M, Kida M, Takekawa N, Namba K, Imada K, Minamino T. 2021. The FlhA linker mediates flagellar protein export switching during flagellar assembly. Commun Biol 4:646.

27. Saijo-Hamano Y, Minamino T, Macnab RM, Namba K. 2004. Structural and functional analysis of the C-terminal cytoplasmic domain of FlhA, an integral membrane component of the type III flagellar protein export apparatus in *Salmonella*. J Mol Biol 343:457–466.

28. Minamino T, Shimada M, Okabe M, Saijo-Hamano Y, Imada K, Kihara M, Namba K. 2010. Role of the C-terminal cytoplasmic domain of FlhA in bacterial flagellar type III protein export. J Bacteriol 192:1929–1936.

29. Shimada M, Saijo-Hamano Y, Furukawa Y, Minamino T, Imada K, Namba K. 2012. Functional defect and restoration of temperature-sensitive mutants of FlhA, a subunit of the flagellar protein export apparatus. J Mol Biol 415:855–865.

30. Kinoshita M, Nakanishi Y, Furukawa Y, Namba K, Imada K, Minamino T. 2016. Rearrangements of α-helical structures of FlgN chaperone control the binding affinity for its cognate substrates during flagellar type III export. Mol Microbiol

101:656–670.

31. Furukawa Y, Inoue Y, Sakaguchi A, Mori Y, Fukumura T, Miyata T, Namba K, Minamino T. 2016. Structural stability of flagellin subunit affects the rate of flagellin export in the absence of FliS chaperone. Mol Microbiol 102:405–416.

32. Minamino T, Morimoto YV, Kinoshita M, Namba K. 2021. Multiple roles of flagellar export chaperones for efficient and robust flagellar filament formation in Salmonella. Front Microbiol 12:756044.

33. Jensen J, Yamini S, Rietsch AR, Spiller BW. 2020. The structure of the type III secretion system export gate with CdsO, an ATPase lever arm. PLOS Pathog 16:e1008923.

34. Schmiger H. 1972. Phage P22 mutants with increased or decreased transduction abilities. Mol Gen Genet 119:75–88.

35. Minamino T, Macnab RM. 1999. Components of the *Salmonella* flagellar export apparatus and classification of export substrates. J Bacteriol 181:1388–1394 (1999).

36. Maier JA, Martinez C, Kasavajhala K, Wickstrom L, Hauser KE. 2015. Simmerling, C., ff14SB: Improving the Accuracy of Protein Side Chain and Backbone Parameters from ff99SB. J Chem Theory Comput 11:3696–3713.

37. Takemura K, Kitao A. 2012. Water model tuning for improved reproduction of rotational diffusion and NMR spectral density. J Phys Chem B 116: 6279–6287.

38. Joung IS, Cheatham TE. 2008. Determination of alkali and halide monovalent ion

parameters for use in explicitly solvated biomolecular simulations. J Phys Chem B 112:9020–9041.

39. Gotz AW, Williamson MJ, Xu D, Poole D, Le Grand S, Walker RC. 2012. Routine microsecond molecular dynamics simulations with AMBER on GPUs. 1. generalized born. J Chem Theory Comput 8:1542–1555.

40. Case DA, Aktulga HM, Belfon K, Ben-Shalom IY, Brozell SR, Cerutti DS, Cheatham TE III, Cisneros GA, Cruzeiro VWD, Darden TA, Duke RE, Giambasu G, Gilson MK, Gohlke H, Goetz AW, Harris R, Izadi S, Izmailov SA, Jin C, Kasavajhala K, Kaymak MC, King E, Kovalenko A, Kurtzman T, Lee TS, LeGrand S, Li P, Lin C, Liu J, Luchko T, Luo R, Machado M, Man V, Manathunga M, Merz KM, Miao Y, Mikhailovskii O, Monard G, Nguyen H, O'Hearn KA, Onufriev A, Pan F, Pantano S, Qi R, Rahnamoun A, Roe DR, Roitberg A, Sagui C, Schott-Verdugo S, Shen J, Simmerling CL, Skrynnikov NR, Smith J, Swails J, Walker RC, Wang J, Wei H, Wolf RM, Wu X, Xue Y, York DM, Zhao S, Kollman PA. 2021. Amber 2021, University of California, San Francisco.

41. Yamaguchi S, Fujita H, Sugata K, Taira T, Iino T. 1984. Genetic analysis of *H2*, the structural gene for phase-2 flagellin in *Salmonella*. J Gen Microbiol 130:255–265.

42. Hara N, Namba K, Minamino T. 2011. Genetic characterization of conserved charged residues in the bacterial flagellar type III export protein FlhA. PLOS ONE 6:e22417.

43. Ohnishi K, Fan F, Schoenhals GJ, Kihara M, Macnab RM. 1997. The FliO, FliP, FliQ, and FliR proteins of *Salmonella typhimurium*: putative components for flagellar assembly. J Bacteriol 179:6092–6099.

44. Kihara M, Minamino T, Yamaguchi S, Macnab RM. 2001. Intergenic suppression between the flagellar MS ring protein FliF of *Salmonella* and FlhA, a membrane component of its export apparatus. J Bacteriol 183:1655–1662.

1 **Table 1. Strains and plasmids used in this study**

Strain/Plasmid	Relevant characteristics	References
Salmonella		
SJW1103	Wild-type for motility and chemotaxis	41
SJW2228	*flhA(G368C)*	27
NH001	Δ*flhA*	42
MMA2228KC	*flhA(G368C/K548C)*	This study
MMA2228FKC	*flhA(G368C/F459C/K548C)*	This study
MMA2228KC-01	*flhA(M365I/G368C/K548C)*	This study
MMA2228KC-02	*flhA(G368C/R370S/K548C)*	This study
MMA2228KC-03	*flhA(G368C/A446E/K548C)*	This study
MMA2228KC-04	*flhA(G368C/K548C/P550S)*	This study
Plasmid		
pTrc99AFF4	Expression vector	43
pMM130	pTrc99AFF4/ FlhA	44
pYI130(G368C)	pTrc99AFF4/ FlhA(G368C)	24
pMKM130(L413A)	pTrc99AFF4/ FlhA(L413A)	This study
pMKM130(G368C/L413A)	pTrc99AFF4/ FlhA(G368C/L413A)	This study
pMKM130(P415A)	pTrc99AFF4/ FlhA(L415A)	This study
pMKM130(G368C/P415A)	pTrc99AFF4/ FlhA(G368C/P415A)	This study
pMKM130(P434A)	pTrc99AFF4/ FlhA(P434A)	This study
pMKM130(G368C/P434A)	pTrc99AFF4/ FlhA(G368C/P434A)	This study
pMKM130(F459A)	pTrc99AFF4/ FlhA(F459A)	This study
pMKM130(G368C/F459A)	pTrc99AFF4/ FlhA(G368C/F459A)	This study
pMKM130(Q477A)	pTrc99AFF4/ FlhA(Q477A)	This study
pMKM130(G368C/Q477A)	pTrc99AFF4/ FlhA(G368C/Q477A)	This study
pMKM130(L492A)	pTrc99AFF4/ FlhA(L492A)	This study
pMKM130(G368C/L492A)	pTrc99AFF4/ FlhA(G368C/L492A)	This study
pMKM130(Q498A)	pTrc99AFF4/ FlhA(Q498A)	This study
pMKM130(G368C/Q498A)	pTrc99AFF4/ FlhA(G368C/Q498A)	This study
pMKM130(K548A)	pTrc99AFF4/ FlhA(K548A)	This study
pMKM130(G368C/K548A)	pTrc99AFF4/ FlhA(G368C/K548A)	This study
pMKM130(P646A)	pTrc99AFF4/ FlhA(P646A)	This study
pMKM130(G368C/P646A)	pTrc99AFF4/ FlhA(G368C/P646A)	This study
pMKM130(P667A)	pTrc99AFF4/ FlhA(P667A)	This study
pMKM130(G368C/P667A)	pTrc99AFF4/ FlhA(G368C/P667A)	This study

2
3

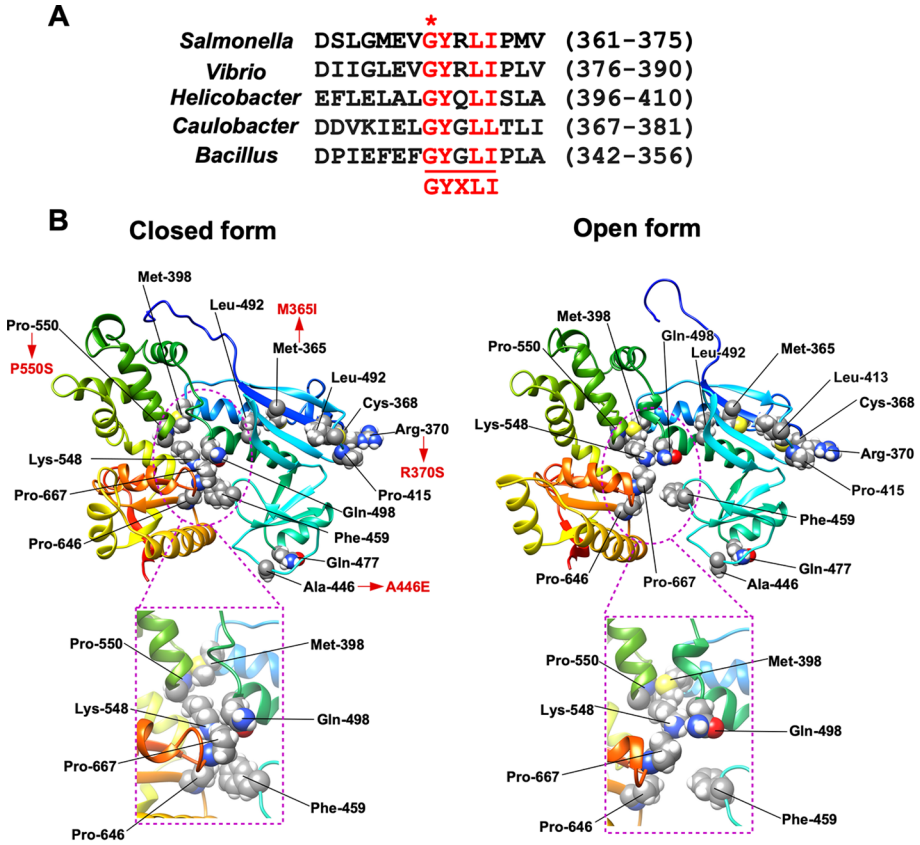

FIG 1. Role of a highly conserved Gly-368 residue of FlhA in dynamic domain motions of FlhA$_C$. (A) Multiple sequence alignments of the conserved GYXLI motif of FlhA homologs. Multiple sequence alignment was carried out by Clustal Omega. Conserved residues are highlighted in red. A highly conserved glycine residue is indicated by an asterisk. UniProt Accession numbers: *Salmonella*, P40729; *Vibrio*, A0A6F8WT44; *Helicobacter*, O06758, *Caulobacter*, Q03845; *Bacillus*, P35620. (B) The closed (left panel) and open (right panel) forms of FlhA$_{C\text{-}G368C}$ obtained by MD simulation. The Cα ribbon diagram of FlhA$_{C\text{-}368C}$ with residues of intragenic suppressor mutations that allow FlhA(G368C) to exert its export function at 42ºC. The intragenic suppressor mutations are highlighted in red. Phe-459 and Gln-498 make hydrophobic contacts with Pro-646 and Pro-667, respectively, in the closed from but not in the open form. The Cα backbone is color-coded from blue to red, going through the rainbow colors from the N- to the C-terminus.

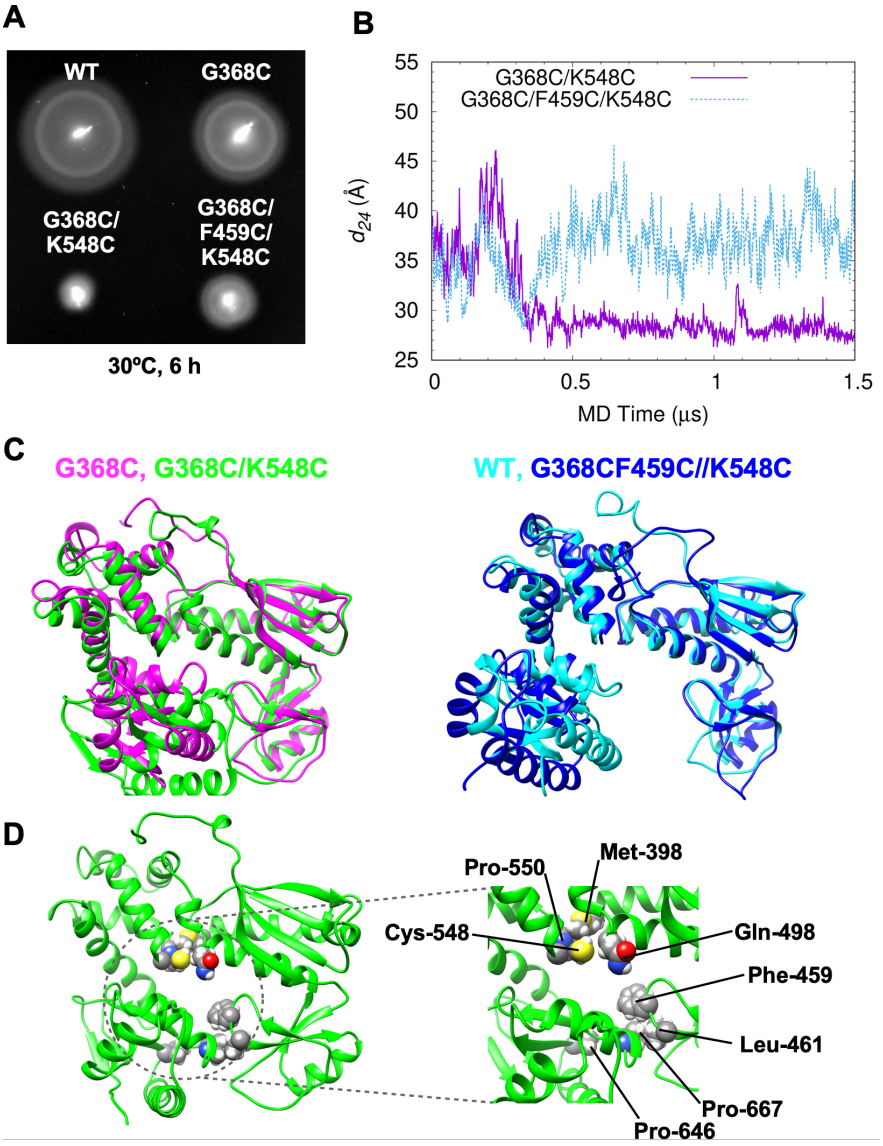

FIG 2. MD simulation of FlhA$_C$ with either G368C/K548C or G368C/F459C/K548C. (A) Motility of SJW1103 (wild type indicated as WT), SJW2228 [*flhA(G368C)* indicated as G368C], MMA2228KC [*flhA(G368C/K548C)* indicated as G368C/K548C] and MMA2228FKC [*flhA(G368C/F459C/K548C)* indicated as G368C/F459C/K548C] in soft agar. Plates were incubated at 30ºC for 6 hours. (B) Center-of-mass distance between domains D2 and D4 (d_{24}) during 1.5 μs MD simulation. (C) Structural comparisons between completely closed forms of FlhA$_{C\text{-}G368C}$ (magenta) and FlhA$_{C\text{-}G368C/K548C}$ (green) (left panels) and between the open forms of wild-type FlhA$_C$ (blue) and FlhA$_{C\text{-}G368C/F459C/K548C}$ (cyan). (D) Interfaces between domains D1 and D3 and between domains D2 and D4 of FlhA$_{C\text{-}G368C/K548C}$.

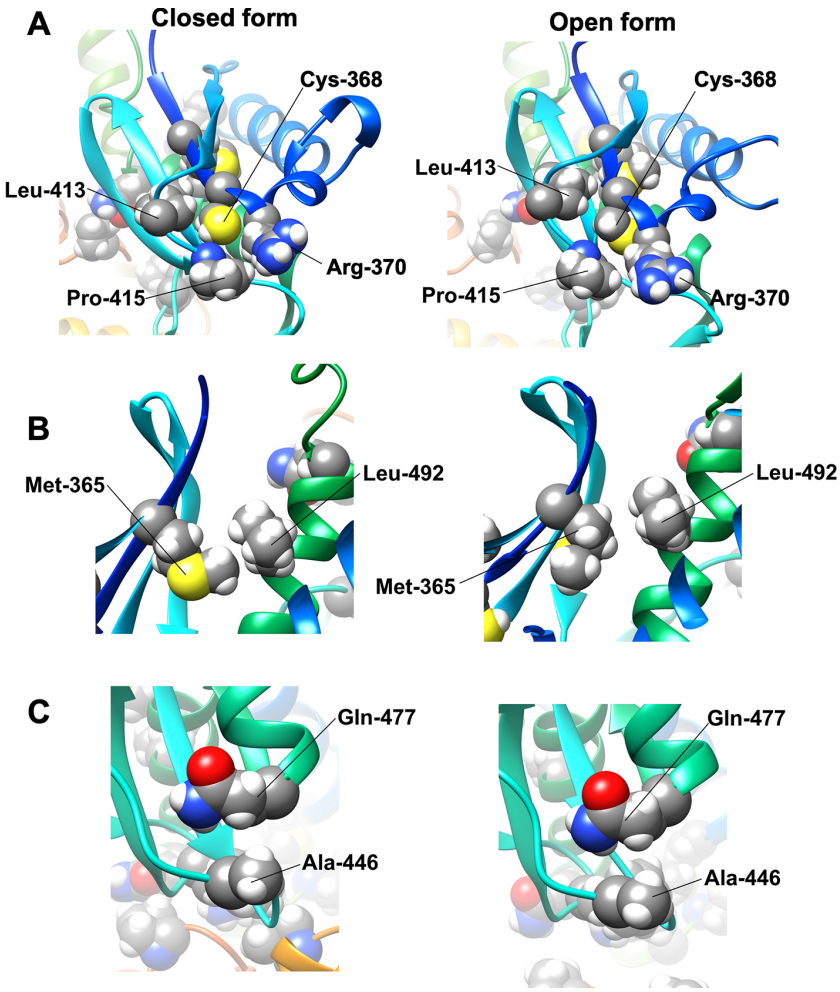

FIG 3. Structural comparison between closed (right panels) and open conformations (right panels) of FlhA$_{C\text{-}G368C}$ obtained by MD simulation. (A) Hydrophobic interactions of Cys-368 with Arg-370, Leu-413, and Pro-415 in the open and closed forms of FlhA$_{C\text{-}G368C}$. (B) Hydrophobic interactions between Met-365 and Leu-492. (C) Interaction between Gln-477 and Ala-446.

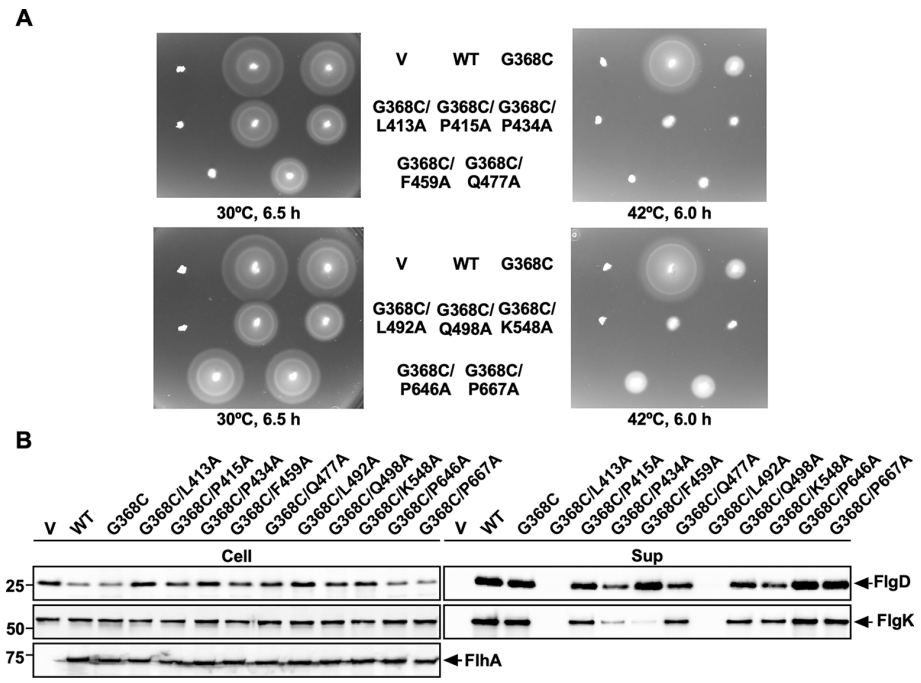

FIG 4. Effect of alanine substitution in residues involved in remodeling of hydrophobic side-chain interaction networks in FlhA$_{C\text{-}G368C}$ on flagellar protein export by the *flhA(G368C)* mutant. (A) Motility of NH001 (Δ*flhA*) carrying pTrc99AFF4 (indicated as V), pMM130 (indicated as WT), pYI130(G368C) (indicated as G368C), pMKM130(G368C/L413A) (indicated as G368C/L413A), pMKM130(G368C/P415A) (indicated as G368C/P415A), pMKM130(G368C/P434A) (indicated as G368C/P434A), pMKM130(G368C/F459A) (indicated as G368C/F459A), pMKM130(G368C/Q477A) (indicated as G368C/Q477A), pMKM130(G368C/L492A) (indicated as G368C/L492A), pMKM130(G368C/Q498A) (indicated as G368C/Q498A), pMKM130(G368C/K548A) (indicated as G368C/K548A), pMKM130(G368C/P646A) (indicated as G368C/P646A) or pMKM130(G368C/P667A) (indicated as G368C/P667A) in 0.35% soft agar. Plates were incubated at 30ºC for 6.5 hours and at 42ºC for 6 hours. (B) Secretion assays of FlgD and FlgK. Immunoblotting, using polyclonal anti-FlgD (1st row), anti-FlgK (2nd row), or anti-FlhA$_C$ (3rd row) antibody, of whole cell proteins (Cell) and culture supernatants (Sup) prepared from the above strains, which were exponentially grown at 30ºC with shaking. The positions of FlgD, FlgK, and FlhA are indicated by arrows. Molecular mass markers (kDa) are shown on the left.

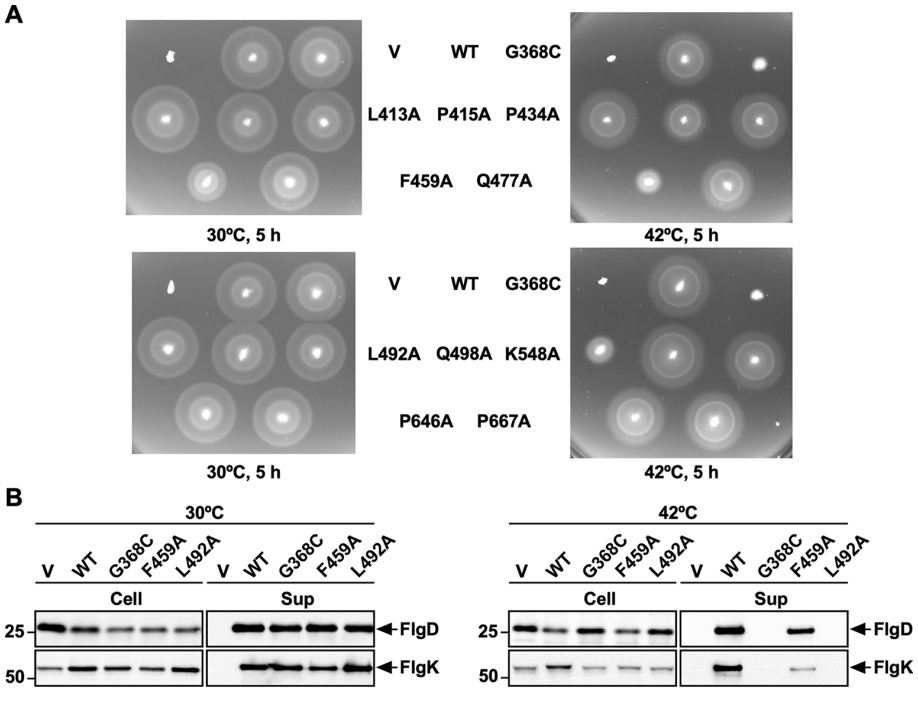

FIG 5. Effect of temperature on the protein export function of FlhA containing a single alanine substitution. (A) Motility of NH001 (Δ*flhA*) carrying pTrc99AFF4 (indicated as V), pMM130 (indicated as WT), pYI130(G368C) (indicated as G368C), pMKM130(L413A) (indicated as L413A), pMKM130(P415A) (indicated as P415A), pMKM130(P434A) (indicated as P434A), pMKM130(F459A) (indicated as F459A), pMKM130(Q477A) (indicated as Q477A), pMKM130(L492A) (indicated as L492A), pMKM130(Q498A) (indicated as Q498A), pMKM130(K548A) (indicated as K548A), pMKM130(P646A) (indicated as P646A)or pMKM130(P667A) (indicated as P667A) in 0.35% soft agar. Plates were incubated at 30ºC and 42ºC for 5 hours. (B) Secretion assays of FlgD and FlgK. Immunoblotting, using polyclonal anti-FlgD (1st row) or anti-FlgK (2nd row) antibody, of whole cell proteins (Cell) and culture supernatants (Sup) prepared from NH001 carrying pTrc99A, pMM130, pYI130(G368C), pMKM130(F459A), or pMKM130(L492A) which were exponentially grown at either 30ºC (left panels) or 42ºC (right panels). The positions of FlgD, and FlgK are indicated by arrows. Molecular mass markers (kDa) are shown on the left.

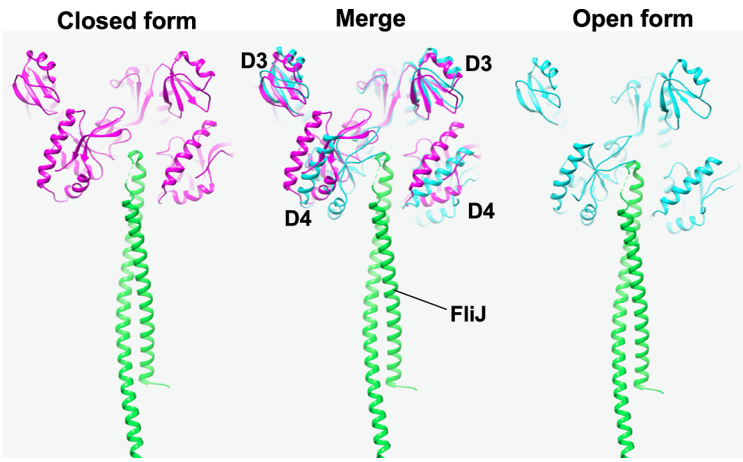

FIG. 6. Model for of the closed (left panel, magenta) and open (right panel, cyan) forms of the FlhA$_C$ ring with FliJ. The ring model was made by fitting domains D1 and D2 of the open form of FlhA$_C$ (PDB ID: 3A5I) and its closed form obtained by MD simulation to those of MxiA$_C$ in the nonameric ring structure (PDB ID: 4A5P). The CdsO-CdsV$_C$ complex structure (PDB ID: 6WA9) was superimposed on the FlhA$_C$ ring models, and then FliJ (green) (PDB ID: 3AJE) was superimposed on the 6WA9 structure to build the FlhA$_C$-FliJ ring complex. Two FlhA$_C$ subunits in the ring model are shown. FliJ can bind to a cleft between domains D4 of neighboring FlhA$_C$ subunits in the open form of the FlhA$_C$ ring (right panel). Because a distance between the D4 domains is longer in the closed form than in the open form (center panel), FliJ presumably cannot bind to the cleft in the closed form.